

Stability region of $K_{0.2}Na_{0.8}AlSi_3O_8$ hollandite at 22 GPa and 2273 K

Youmo Zhou¹  · Tetsuo Irifune^{1,2} · Hiroaki Ohfuji¹ · Toru Shinmei¹ · Wei Du^{1,2}

Received: 6 May 2016 / Accepted: 28 July 2016 / Published online: 11 August 2016
© Springer-Verlag Berlin Heidelberg 2016

Abstract Lingunite (hollandite with Na contents of 80–85 mol%) discovered in the shock veins of strongly shocked meteorites is an important signature of shock metamorphism. To seek the stability region of lingunite, phase relations in the system $KAlSi_3O_8$ – $NaAlSi_3O_8$ have been investigated by multi-anvil experiments at pressures of 20–23 GPa and temperatures of 1873 and 2273 K. Phase assemblages of hollandite + jadeite + stishovite, hollandite + calcium ferrite-type $NaAlSiO_4$ + stishovite and hollandite single phase have been recovered, depending on the pressure–temperature conditions and the compositions of starting materials. Both pressure and temperature have large effects on the solubility of Na in hollandite, and hollandite with 79 mol% Na, similar to the natural lingunite in terms of Na content, has been firstly synthesized at 22 GPa and 2273 K. The stability region of $K_{0.2}Na_{0.8}AlSi_3O_8$ hollandite is comparable to the typical pressure–temperature conditions of the shock veins of strongly shocked meteorites (20–25 GPa and 2273–2500 K).

Keywords Hollandite · Lingunite · Phase relation · High pressure and high temperature

Introduction

$KAlSi_3O_8$ hollandite, which has been named liebermanite recently (Ma et al. 2015), is known as the high-pressure polymorph of orthoclase (Ringwood et al. 1967; Urakawa et al. 1994). It is also shown that plagioclase underwent shock metamorphism and transformed to the hollandite structure in some strongly shocked meteorites (shock stage S5–S6, Stöffler et al. 1991) (e.g., Gillet et al. 2000; Tomioka et al. 2000). The shock-metamorphic hollandite discovered in strongly shocked meteorites is important for understanding the petrogenesis and the pressure–temperature (P–T) history of meteorites, among which the hollandite containing 80–85 mol% Na is the most common category and has been named lingunite (Liu and El Goresy 2007). Lingunite has been frequently observed in the shock veins of strongly shocked meteorites, having chemical compositions similar to those of maskelynite and the original plagioclase (e.g., Gillet et al. 2000; Tomioka et al. 2000; Ohtani et al. 2004; Ozawa et al. 2009).

In contrast to the frequent discovery of lingunite in meteorites, hollandite with Na contents higher than 50 mol% has not been synthesized yet. To make clear definitions, hereafter, mineral names of “K and Na hollandite” refer to $KAlSi_3O_8$ and $NaAlSi_3O_8$ hollandite end-members, respectively, while “hollandite” represents their solid solutions, and “lingunite” is the hollandite discovered in meteorites, which contains 80–85 mol% Na. Although Liu (1978) and Tutti (2007) identified trace Na hollandite in the albitic compositions heated by laser in diamond anvil cells (DAC) around 22 GPa at 1273 and 2273 K, respectively, based on a few fuzzy XRD peaks which could be indexed to the hollandite structure, the weak “hollandite” peaks and the tremendous amount of coexisting phases debase their

✉ Youmo Zhou
zhouyoumo201637@gmail.com

¹ Geodynamics Research Center, Ehime University,
Matsuyama 790-8577, Japan

² Earth-Life Science Institute, Tokyo Institute of Technology,
Tokyo 152-8550, Japan

conclusions about the stability region of Na hollandite. On the other hand, the phase relations of $\text{NaAlSi}_3\text{O}_8$ reported by Yagi et al. (1994) and Akaogi et al. (2010) demonstrate that Na hollandite cannot be stabilized around 22 GPa at 1073–2273 K, which contradicts the stability region of Na hollandite claimed by Liu (1978), Liu and El Goresy (2007) and Tutti (2007) at similar P–T conditions.

The solubility of Na in hollandite also has been previously studied in the system KAlSi_3O_8 – $\text{NaAlSi}_3\text{O}_8$. Yagi et al. (1994) reported that the solubility of Na in hollandite is about 40 mol% at 22.5 GPa and 1273 K. Liu (2006) studied the system KAlSi_3O_8 – $\text{NaAlSi}_3\text{O}_8$ at 14–25 GPa and 1673–2673 K and emphasized that the solubility of Na in hollandite positively correlates to temperature. However, according to Liu (2006), the solubility of Na in hollandite does not exceed 40 mol% at 14–25 GPa and 1673–2073 K, which is contradictory to the results of Yagi et al. (1994). Moreover, according to Liu (2006), the solubility of Na in hollandite at 14–25 GPa does not exceed 25 and 41 mol% at 1673 and 2073 K, respectively, while Akaogi et al. (2005) and Liu et al. (2005) synthesized hollandite with Na contents of 40–50 mol% at 22 GPa and temperatures of 1673 and 1973 K, respectively. In addition, Ishii et al. (2012) reported the solubility of Na in the hollandite involved in the phase assemblages of continental crust at 20–27 GPa and 1673–2073 K, and the maximal solubility of Na in hollandite encountered at 22 GPa and each temperature (31 mol%, 1673 K; 41 mol%, 1873 K; 45 mol%, 2073 K) is higher than those of Liu (2006) at similar P–T conditions (25 mol%, 1673 K; 30 mol%, 1873 K; 41 mol%, 2073 K).

Due to the above-mentioned discrepancies between Liu (2006) and other previous studies, the solubility of Na in hollandite needs further investigation, especially at high temperatures. To clarify the effects of pressure and temperature on the solubility of Na in hollandite, we re-examined the phase relations in the system KAlSi_3O_8 – $\text{NaAlSi}_3\text{O}_8$ via multi-anvil experiments, particularly focusing those at pressures of 20–23 GPa and temperatures of 1873 and 2273 K.

Experimental methods

Feldspathic glasses with compositions of $\text{K}_{0.45}\text{Na}_{0.55}\text{AlSi}_3\text{O}_8$ and $\text{K}_{0.2}\text{Na}_{0.8}\text{AlSi}_3\text{O}_8$ were used as starting materials for high-pressure and high-temperature (HPHT) experiments. To prepare compositionally homogeneous glasses, mixtures of stoichiometrically weighed chemicals, K_2CO_3 (>99.5 %, Kanto Chemical Co., Inc.), Na_2CO_3 (>99.5 %, Kanto Chemical Co., Inc.), Al_2O_3 (>99.0 %, Kanto Chemical Co., Inc.) and SiO_2 (99.9 %, Kojundo Chemical Laboratory Co., Ltd), were firstly decarbonated at 1273 K for 12 h and then melted twice in Pt crucibles at 2000 K for 1 h.

About 15 mol% K_2CO_3 was added into the chemical mixtures in advance to compensate the loss of K during heating. Transparent glasses were obtained by air quenching, and their compositions were found to be consistent with the designed stoichiometries within analytic uncertainties by electron probe microanalysis. The glasses were finely ground, stored at 383 K and sealed in Pt capsules before HPHT experiments.

Experimental runs were performed at pressures of 20–23 GPa and temperatures of 1873 and 2273 K in the Kawai-type multi-anvil apparatuses (Orange 1000 and 2000) installed at Geodynamics Research Center (GRC), Ehime University. A 10/4 (octahedron edge length/truncation edge length) cell assembly with a LaCrO_3 tubular heater was adopted, and MgO and ZrO_2 were used as electrical and thermal insulators surrounding Pt capsules and Mo electrodes, respectively. Pressures at room temperature were calibrated by the diagnostic changes in the electrical resistances of ZnTe (9.6 and 12.0 GPa), ZnS (15.5 GPa), GaAs (18.3 GPa) and GaP (23.0 GPa) induced by the semiconductor–metal phase transitions at high pressures. Pressures at 1873 K were estimated by the phase transitions of Mg_2SiO_4 between forsterite and wadsleyite at 15.0 GPa (Morishima et al. 1994), Mg_2SiO_4 between wadsleyite and ringwoodite at 21.4 GPa (Suzuki et al. 2000) and MgSiO_3 between akimotoite and bridgmanite at 22.3 GPa (Fei et al. 2004). Pressures at 2273 K were estimated by the phase transition of MgSiO_3 between majorite and bridgmanite at 21.5 GPa (Fei et al. 2004) and the decomposition of Mg_2SiO_4 into bridgmanite and periclase at 23 GPa (Fei et al. 2004). Temperature was monitored by a W_{97}Re_3 – $\text{W}_{75}\text{Re}_{25}$ thermocouple. No correction was made for the pressure effect on the electromotive force of the thermocouple.

In most of the HPHT experiments, temperature was increased to the target value within 20 min, and the heating was kept for 12 h and subsequently stopped by cutting off the power supply. We found that compositional zoning usually occurs in the hollandite grains when heating durations are relatively short (e.g., 2 h) in the HPHT experiments above 20 GPa, while the samples heated for 12 h comprise compositionally homogeneous grains with sharp boundaries, indicating that the adopted duration of 12 h in most of the present runs is sufficient to achieve phase equilibrium. Conditions and results of the representative HPHT experiments are summarized in Table 1.

Recovered samples were embedded in epoxy resin and polished for subsequent measurements. Because of their small sizes, the phase assemblages were investigated by a micro-focus X-ray diffractometer (Rigaku MicroMax-007HF) using $\text{Cu K}\alpha$ radiation. Lattice parameters of hollandite were calculated using 10–25 peaks in a two-theta range from 15° to 100°. Polycrystalline Si was used as an

Table 1 Experimental conditions and results

Run no.	Pressure (GPa)	Duration (h)	Starting material	Product
T = 1873 K				
OD1426	15.0	3	K80	Holl, Jd, St
			K45	Holl, Jd, St
OS2771	21.4	12	K45	Holl, Jd, St
			K20	Holl, Jd, St
OD1436	22.1	3	K45	Holl, Jd, St
OS2743	23.0	12	K45	Holl, CF, St
			K20	Holl, CF, St
T = 2273 K				
OS2720	20.5	12	K45	Holl, Jd, St
			K20	Holl, Jd, St
OS2712*	21.4	9	K45	Holl, tr. St
			K20	Holl, Jd, St
OS2735	22.0	12	K45	Holl, tr. St
			K20	Holl, tr. St
OS2731	22.5	12	K45	Holl, tr. St
			K20	Holl, CF, St
OS2729	23.0	12	K20	Holl, CF, St

K80, $K_{0.8}Na_{0.2}AlSi_3O_8$; K45, $K_{0.45}Na_{0.55}AlSi_3O_8$; K20, $K_{0.2}Na_{0.8}AlSi_3O_8$

Holl hollandite, Jd jadeite, CF calcium ferrite-type $NaAlSiO_4$, St stishovite, tr. trace

* In Run OS2712, an 8/3 cell assembly with individual pressure calibrations was used

external standard to calibrate the peak positions of the XRD patterns. For electron microscopic observation and compositional analysis, the samples were coated with osmium. In the case of carbon coating, the uncertainty in the thickness of the coating layer can cause the variation in the quantitative values for elements and the weight total, while this variation can be reduced by using osmium coating instead, because the thickness of osmium coating layer can be precisely controlled, which enables precious absorption corrections for the coating layer (Ohfuji and Yamamoto 2015). The micro-textures were observed with a field-emission scanning electron microscope (FESEM, JEOL JSM7000F), and the chemical compositions were measured by an energy dispersive X-ray spectrometer (EDS, Oxford Instruments X-Max^N) attached to the FESEM with working parameters of 15 kV, 1 nA and collection times of 30–50 s. Albite was used as the standard for Na, Al and Si, and adularia was used for K. To avoid the serious evaporation of K and Na from the irradiated samples, compositional analysis in area mode was selected when measuring the feldspar standards and the starting materials, and point analysis was chosen when measuring the recovered samples. The EDS data were processed by the software Aztec (version

2.4, Oxford Instruments Nanotechnology Tools Ltd) using the XPP method. The compositions of hollandite showed ideal stoichiometries of $(K,Na)AlSi_3O_8$, but the weight totals were always about 2 % higher than 100 %. This is probably due to the sharp contrast in density between hollandite (3.89 g/cm^3 , Nishiyama et al. 2005) and feldspar ($2.55\text{--}2.65 \text{ g/cm}^3$), which causes different emission and absorption of characteristic X-rays in the hollandite and feldspar samples. To solve this problem, K hollandite was synthesized and used as the standard for K, Al and Si. The ion numbers of hollandite quantified using the different standards (feldspars and K hollandite) are identical, and the weight totals can be corrected using the synthetic K hollandite as the standard. The compositions of hollandite and some other phases (jadeite, calcium ferrite-type $NaAlSiO_4$ and stishovite) are given in Tables 2 and 3, respectively.

Results and discussion

Figure 1 shows the micro-textures of some typical samples with bulk compositions of $K_{0.2}Na_{0.8}AlSi_3O_8$. K-bearing hollandite can be recognized through its high brightness and elongated shape, while jadeite, calcium ferrite-type $NaAlSiO_4$ (CF) and stishovite look darker. Jadeite behaves as a matrix with inserted crystals of hollandite and stishovite in the phase assemblage of hollandite + jadeite + stishovite (Fig. 1a, d). In Fig. 1b, except hollandite and one marked grain of CF, the matrix is dominated by tiny stishovite and CF, grain boundaries of which are hardly recognizable. Figure 1c is a magnification of the same sample shown in Fig. 1b, revealing a texture composed of sub-micron stishovite and nano-sized CF. The duration of 12 h is insufficient to promote the grain growth of CF and stishovite at 23 GPa and 1873 K. Yagi et al. (1994) and Akaogi et al. (2010) also observed fine crystals of CF in their samples recovered at 23 GPa below 1873 K. The grains of CF synthesized at 2273 K have sizes up to $10 \mu\text{m}$, as shown in Fig. 1f. Comparing Fig. 1a, b with Fig. 1d, f, respectively, it can be seen that the volume fraction of hollandite increases with increasing the temperature from 1873 to 2273 K at a fixed pressure, which is attributed to the fact that the hollandite obtained at 2273 K contains more Na than those obtained at 1873 K at a fixed pressure (Table 2).

XRD patterns of some typical samples are shown in Fig. 2, including the three typical phase assemblages obtained in our HPHT experiments. High-pressure phase relations in the system $KAlSi_3O_8\text{--}NaAlSi_3O_8$ at 1873 and 2273 K (Fig. 3a, b) are modally consistent with those at 1273 K (Yagi et al. 1994): hollandite + jadeite + stishovite below 22 GPa, hollandite + CF + stishovite above 22 GPa and hollandite in the single-phase region; the solubility of Na in hollandite increases with increasing pressure up to

Table 2 Compositions of hollandite

Run no.	P (GPa)	SM	K ₂ O	Na ₂ O	Al ₂ O ₃	SiO ₂	Total (wt%)	K	Na	Al	Si	ΣCation*	Na/(K + Na)
T = 1873 K													
OD1426	15.0	K80	15.25(28)	1.01(13)	18.05(22)	66.10(43)	100.41(60)	0.89(2)	0.09(1)	0.97(1)	3.02(1)	4.98(1)	0.09(1)
		K45	14.95(34)	1.07(17)	17.66(21)	66.79(55)	100.49(73)	0.87(2)	0.09(1)	0.95(1)	3.05(1)	4.96(1)	0.10(1)
OS2771	21.4	K45	11.32(44)	3.77(28)	18.50(25)	65.74(80)	99.33(93)	0.66(3)	0.33(2)	1.00(1)	3.00(1)	4.99(1)	0.34(2)
		K20	10.59(43)	4.10(37)	18.47(22)	65.58(55)	98.74(63)	0.62(3)	0.36(3)	1.00(1)	3.01(1)	4.99(1)	0.37(3)
OD1436	22.1	K45	8.56(25)	5.87(20)	18.68(24)	67.62(58)	100.74(76)	0.49(1)	0.51(2)	0.98(1)	3.02(1)	4.99(1)	0.51(1)
OS2743	23.0	K45	11.96(74)	3.46(51)	18.74(21)	65.86(39)	100.03(47)	0.69(4)	0.31(4)	1.00(1)	3.00(1)	5.00(1)	0.31(4)
		K20	11.85(70)	3.29(56)	18.60(30)	66.66(47)	100.40(74)	0.68(4)	0.29(5)	0.99(1)	3.01(1)	4.98(1)	0.30(5)
T = 2273 K													
OS2720	20.5	K45	9.44(52)	5.00(38)	18.19(19)	66.11(34)	98.74(44)	0.55(3)	0.44(3)	0.98(1)	3.02(1)	4.99(1)	0.45(3)
		K20	9.80(29)	4.71(23)	18.18(32)	66.31(41)	99.00(54)	0.57(2)	0.42(2)	0.98(1)	3.02(1)	4.98(1)	0.42(2)
OS2712	21.4	K45	7.90(19)	6.01(16)	18.51(07)	66.26(39)	98.68(50)	0.46(1)	0.53(1)	0.99(0)	3.01(1)	4.99(2)	0.54(0)
		K20	5.13(89)	8.24(61)	18.75(20)	66.88(35)	98.99(36)	0.29(5)	0.72(5)	0.99(1)	3.00(1)	5.01(1)	0.71(5)
OS2735	22.0	K45	8.39(17)	6.08(18)	18.86(19)	67.37(40)	100.70(54)	0.48(1)	0.53(1)	0.99(1)	3.01(1)	5.00(1)	0.52(1)
		K20	3.85(10)	9.38(23)	19.16(15)	68.58(34)	100.98(40)	0.22(1)	0.80(2)	0.99(1)	3.01(1)	5.01(1)	0.79(1)
OS2731	22.5	K45	8.72(18)	5.78(18)	18.78(22)	66.80(36)	100.08(49)	0.50(1)	0.50(1)	0.99(1)	3.00(1)	5.00(1)	0.50(1)
		K20	6.53(76)	7.39(57)	18.95(23)	67.45(43)	100.33(52)	0.37(4)	0.64(5)	0.99(1)	3.00(1)	5.00(1)	0.63(4)
OS2729	23.0	K20	8.77(58)	5.63(41)	19.07(19)	66.69(49)	100.18(51)	0.50(3)	0.49(4)	1.01(1)	2.99(1)	5.00(1)	0.49(3)

SM starting materials, see Table 1

* Oxygen number is fixed to 8

Table 3 Compositions of jadeite, calcium ferrite-type NaAlSiO₄ and stishovite

Run no.	P (GPa)	SM	Phase	Na ₂ O	Al ₂ O ₃	SiO ₂	Total (wt%)	O (fixed)	Na	Al	Si	ΣCation	
T = 2273 K													
OS2720	20.5	K45	Jd	15.19(34)	25.56(13)	59.51(34)	100.26(79)	6	0.99(1)	1.01(1)	1.99(1)	4.00(1)	
			St	–	0.86(31)	100.57(34)	101.44(13)	2	–	0.01(0)	0.99(0)	1.00(0)	
			K20	Jd	15.22(9)	25.56(37)	60.57(36)	101.36(22)	6	0.98(1)	1.00(1)	2.01(1)	3.99(1)
				St	–	1.39(18)	99.78(14)	101.17(26)	2	–	0.02(0)	0.99(0)	1.00(0)
OS2731	22.5	K20	CF	21.83(33)	35.81(45)	42.72(43)	100.36(32)	4	1.00(1)	0.99(1)	1.01(1)	3.00(1)	
			St	–	1.54(18)	99.66(26)	101.19(37)	2	–	0.02(0)	0.99(0)	1.01(0)	
OS2729	23.0	K20	CF	21.47(31)	36.54(45)	41.63(16)	99.64(70)	4	0.99(1)	1.02(1)	0.99(0)	3.00(1)	
			St	–	1.15(11)	99.85(51)	101.00(49)	2	–	0.01(0)	0.99(0)	1.00(0)	

SM starting materials, see Table 1. *Jd* jadeite, *CF* calcium ferrite-type NaAlSiO₄, *St* stishovite

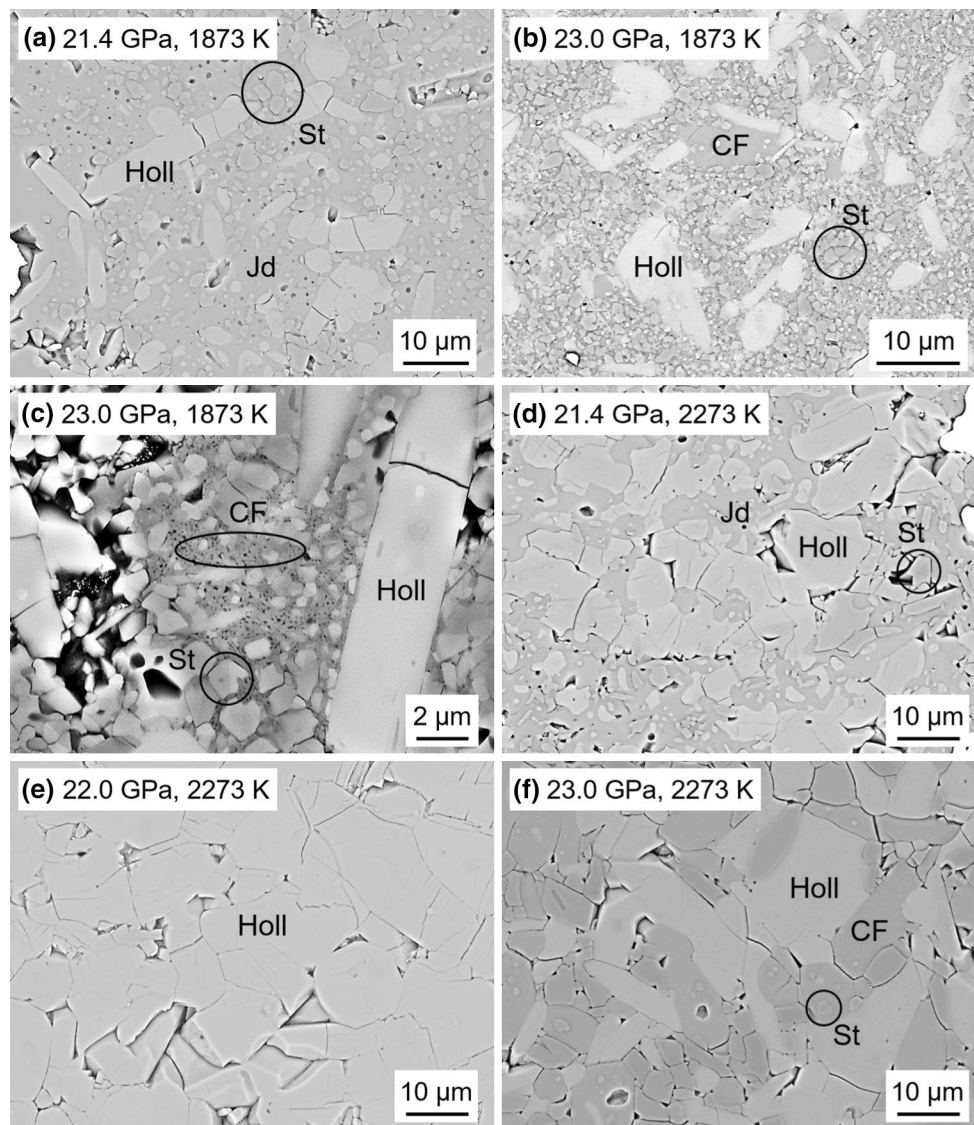
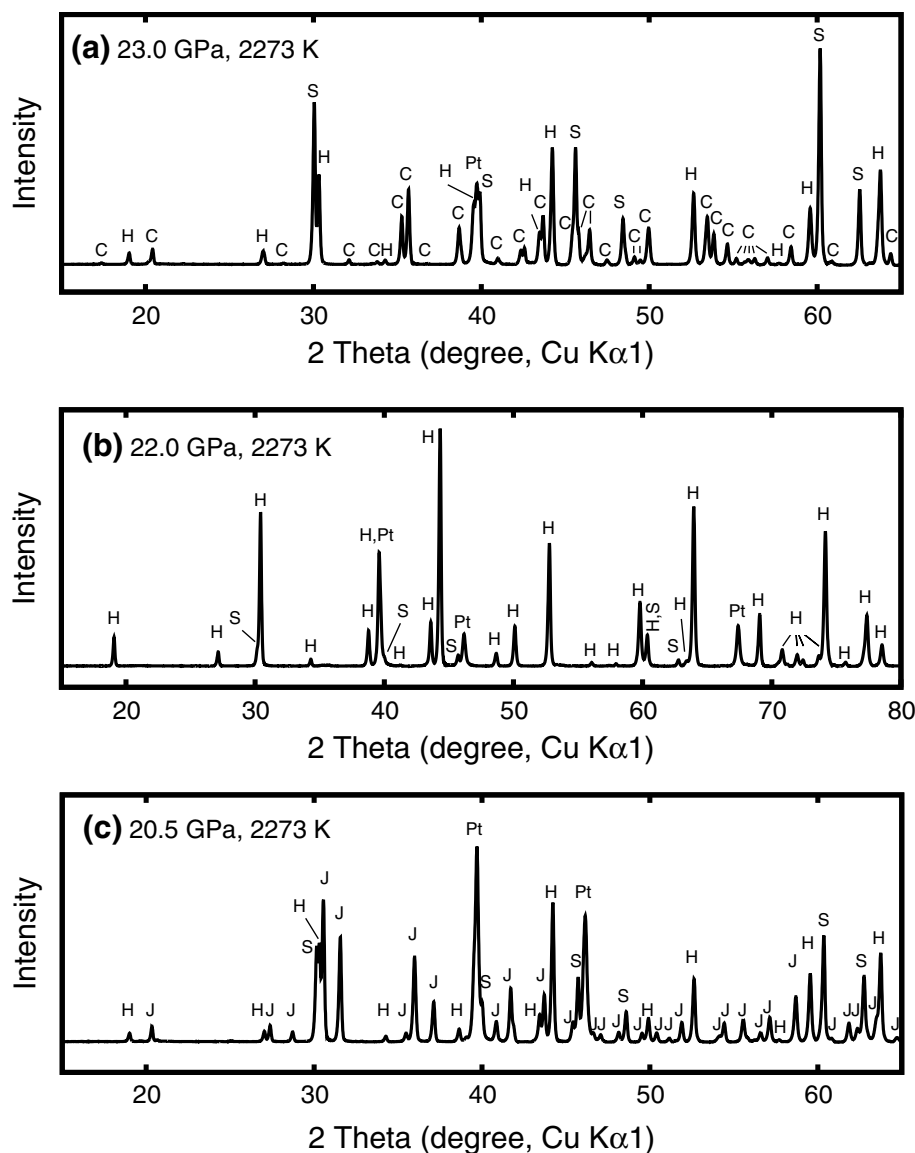


Fig. 1 Back-scattered electron images of some typical samples with bulk compositions of $K_{0.2}Na_{0.8}AlSi_3O_8$ synthesized at: **a** 21.4 GPa, 1873 K (OS2771); **b** 23.0 GPa, 1873 K (OS2743); **c** 23.0 GPa, 1873 K (OS2743, high-magnification observation of the same sam-

ple shown in **b**); **d** 21.4 GPa, 2273 K (OS2712); **e** 22.0 GPa, 2273 K (OS2735); **f** 23.0 GPa, 2273 K (OS2729). *Holl* hollandite, *Jd* jadeite, *CF* calcium ferrite-type NaAlSiO₄, *St* stishovite

Fig. 2 XRD patterns of some typical samples with bulk compositions of $K_{0.2}Na_{0.8}AlSi_3O_8$ synthesized at: **a** 23.0 GPa, 2273 K (OS2729); **b** 22.0 GPa, 2273 K (OS2735); **c** 20.5 GPa, 2273 K (OS2720). *H* hollandite, *J* jadeite, *C* calcium ferrite-type $NaAlSiO_4$, *S* stishovite, *Pt* platinum (capsule material). Pt capsules were involved in the XRD measurements, because of the small sizes of the samples



22 GPa, while it decreases substantially after the dissociation of jadeite into CF and stishovite, because the calcium ferrite structure is more capable of accommodating Na than the hollandite structure (Yamada et al. 1984). Figure 3c shows a positive temperature dependence of the solubility of Na in hollandite, in addition to the equally significant pressure effect that the solubility of Na in hollandite varies substantially in the pressure range from 20 to 23 GPa, and the dissociation of jadeite into CF and stishovite changes the change trend of the solubility of Na in hollandite from increase to decrease. The hollandite synthesized at 22 GPa and 2273 K using the $K_{0.2}Na_{0.8}AlSi_3O_8$ glass (Fig. 1e) is almost a single phase with 79 mol% Na, similar to lingunite in terms of Na content, and its XRD pattern (Fig. 2b) shows the existence of stishovite in trace amount. Jadeite dissociates into CF and stishovite at about 22 GPa at 1873

and 2273 K, which agrees with the experimental results of Akaogi et al. (2010). However, the Clapeyron slope is not discussed in this study, since more accurate data are needed to confirm the plausible temperature dependence of jadeite dissociation (Yagi et al. 1994; Akaogi et al. 2010). According to the compositional analysis (Table 3), jadeite and CF are almost stoichiometric, and the K content in jadeite and CF is below the detection limit; stishovite contains a small amount of Al_2O_3 (<2 wt%).

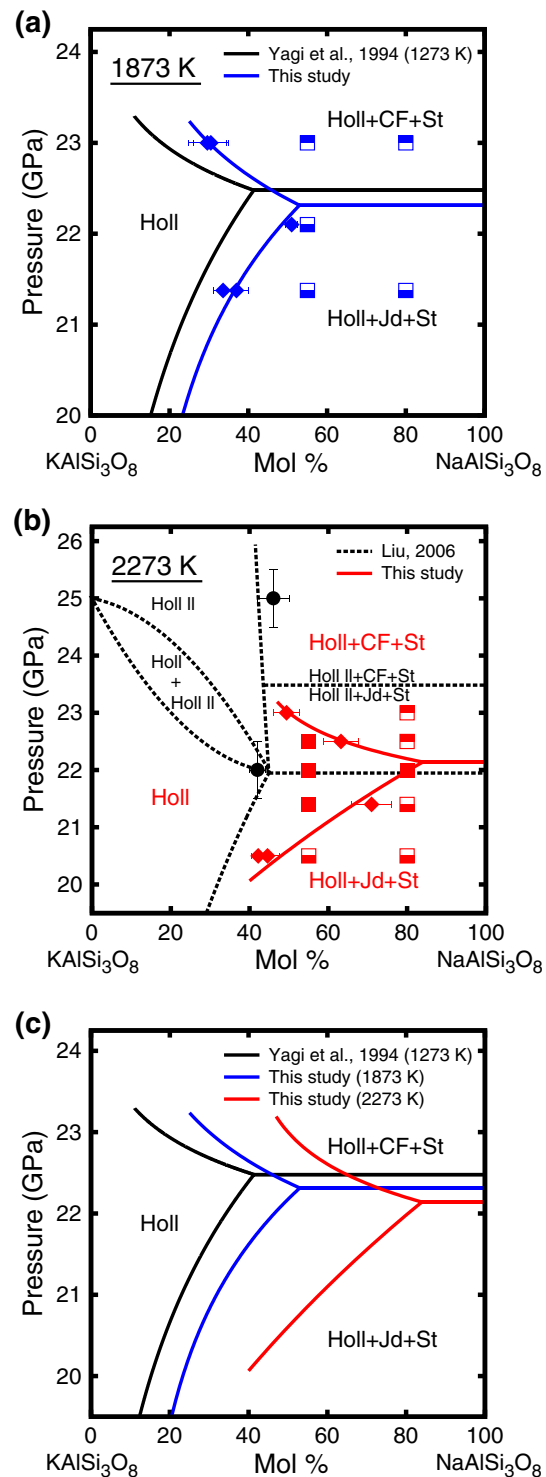
Considering the positive temperature dependence shown in Fig. 3c, Na hollandite is likely stable around 22 GPa only at temperatures above 2273 K. It is possible that the Na hollandite noticed by Liu (1978) and Tutti (2007) in their DAC experiments was formed locally at some hot spots of laser heating where the temperatures were underestimated. Kawai and Tsuchiya (2013) predicted that Na hollandite is

Fig. 3 High-pressure phase relations in the system KAISi_3O_8 – $\text{NaAlSi}_3\text{O}_8$ at **a** 1873 and **b** 2273 K and **c** phase boundaries in the system KAISi_3O_8 – $\text{NaAlSi}_3\text{O}_8$ at different temperatures. Squares with the lower and upper parts filled represent the phase assemblages of hollandite (Holl) + jadeite (Jd) + stishovite (St) and hollandite + calcium ferrite-type $\text{NaAlSi}_3\text{O}_8$ (CF) + stishovite, respectively; solid squares, hollandite single phase. Diamonds reflect the compositions of hollandite coexisting with other phases. In **b**, the black circles and the dashed phase boundaries marked by black texts are based on the results of Liu (2006), while the phase relations obtained in this study are denoted by red texts. Liu (2006) omitted the loops of “Holl I + Holl II” at other temperatures rather than 1673 K in his diagram for clearance. Thus, to completely show the phase relations of Liu (2006), the loop of “Holl I + Holl II” is added to his results in **b**. It should be pointed out that this loop shows only phase relations but nothing accurate about compositions and pressures

metastable based on theoretical calculations, although their calculations were conducted at 0 K.

Figure 3b shows that our results are quite different from those of Liu (2006). The data of Liu (2006) may match our data, if the former moves down to lower pressures. This discrepancy is likely due to the fact that Liu (2006) did not do pressure calibration at high temperatures. Liu (2006) suggested that pressure is unimportant to the solubility of Na in hollandite at 22 and 25 GPa, because the latter shows no large variation at 1673–2273 K in his study. However, it can be seen from the results of Liu (2006) that the phase assemblage of “hollandite II” (to be discussed later) + jadeite + stishovite at 22 GPa is replaced by the phase assemblage of “hollandite II” + CF + stishovite at 25 GPa. Using two data across a pressure interval of 3 GPa, Liu (2006) did not find the substantial change of the solubility of Na in hollandite before and after the dissociation of jadeite into CF and stishovite, which can be seen in Yagi et al. (1994), Ishii et al. (2012) and this study (Fig. 3), and therefore underestimated the solubility of Na in hollandite. In this study, the pressures of HPHT experiments were estimated based on the widely studied phase relations of Mg_2SiO_4 and MgSiO_3 , and the phase relations in the system KAISi_3O_8 – $\text{NaAlSi}_3\text{O}_8$ have been carefully investigated in the pressure range from 20 to 23 GPa, within which the maximal solubility of Na in hollandite is encountered at each temperature, according to previous studies (Yagi et al. 1994; Liu 2006; Ishii et al. 2012). As a result, the pressure effect on the solubility of Na in hollandite has been clarified, and $\text{K}_{0.2}\text{Na}_{0.8}\text{AlSi}_3\text{O}_8$ hollandite has been synthesized.

K hollandite transforms to a monoclinic structure named hollandite II (Sueda et al. 2004) via a second-order phase transition around 20 GPa at room temperature (Ferroir et al. 2006). Liu (2006) hypothetically modified the phase relations in the system KAISi_3O_8 – $\text{NaAlSi}_3\text{O}_8$ by taking this phase transition into account, but no evidence was given to prove the occurrence of the unquenchable hollandite II phase in his products recovered from HPHT, and the effects



of temperature and Na substitution on the phase transition were out of consideration. According to the Clapeyron slope measured by Nishiyama et al. (2005), the pressures of the previous (Yagi et al. 1994; Liu 2006) and present experiments are not high enough to trigger the hollandite–hollandite II phase transition at high temperatures. On the other hand, the effect of Na substitution was studied merely by

Table 4 Lattice parameters and unit cell volumes of hollandite

Na content (mol%)	a (Å)	c (Å)	V (Å ³)	Run no.	SM
0	9.3264(2)	2.7274(1)	237.24(1)		
9	9.3207(3)	2.7246(2)	236.70(2)	OD1426	K80
10	9.3208(4)	2.7246(3)	236.71(4)	OD1426	K45
34	9.3073(3)	2.7207(2)	235.68(3)	OS2771	K45
37	9.3045(5)	2.7199(3)	235.47(4)	OS2771	K20
42	9.3003(7)	2.7189(4)	235.17(6)	OS2720	K20
45	9.2994(3)	2.7189(2)	235.13(3)	OS2720	K45
49	9.2929(3)	2.7184(1)	234.75(2)	OS2729	K20
50	9.2902(2)	2.7181(1)	234.59(1)	OS2731	K45
52	9.2890(5)	2.7176(3)	234.49(4)	OS2735	K45
54	9.2865(2)	2.7182(1)	234.42(1)	OS2712	K45
63	9.2733(4)	2.7174(2)	233.68(4)	OS2731	K20
71	9.2767(7)	2.7169(3)	233.81(6)	OS2712	K20
79	9.2623(6)	2.7147(3)	232.90(4)	OS2735	K20

SM starting materials, see Table 1

some theoretical calculations (Boffa Ballaran et al. 2009; Caracas and Boffa Ballaran 2010; Kawai and Tsuchiya 2013) and remains unclear. Since the effects of temperature and Na substitution on the hollandite–hollandite II phase transition are unclear in the system KAlSi_3O_8 – $\text{NaAlSi}_3\text{O}_8$, we hesitate to accept (1) the phase relations reported by Liu (2006) and (2) the maximal solubility of Na in hollandite estimated by Liu (2006) based on the hollandite–hollandite II phase transition at 20–25 GPa and 1673–2273 K. Here, we show the phase relations without the hollandite II phase, based on the phase identification of the samples recovered from HPHT. Studies using in situ X-ray observation are needed to further explore this issue.

Lattice parameters and unit cell volumes of hollandite are listed in Table 4 and plotted as functions of Na content in Fig. 4. The lengths of a, c axes and the unit cell volume decrease with increasing Na content in hollandite, because of replacing K (ionic radius, 1.33 Å) by relatively smaller Na (ionic radius, 0.95 Å). The lattice parameters and unit cell volumes of hollandite given by linear fittings are $a = 9.3302(22) - 0.0795(45) \times X_{\text{Na}}$ Å, $c = 2.7260(4) - 0.0147(9) \times X_{\text{Na}}$ Å and $V = 237.303(94) - 5.297(196) \times X_{\text{Na}}$ Å³, where X_{Na} is $\text{Na}/(\text{K} + \text{Na})$. Figure 4 shows that the lattice parameters of K hollandite in this study agree with those in Yagi et al. (1994), but the extrapolations of lattice parameters to Na hollandite in this study deviate from those in Yagi et al. (1994). Analytic uncertainties of XRD measurements likely affect their results, since only four data of lattice parameters of hollandite with Na contents lower than 40 mol% were used for the linear regression. Lattice parameters of the $\text{Na}_{0.80}\text{Ca}_{0.12}\text{K}_{0.08}\text{Al}_{1.12}\text{Si}_{2.88}\text{O}_8$ lingunite (Gillet et al. 2000) are also plotted in Fig. 4 for comparison.

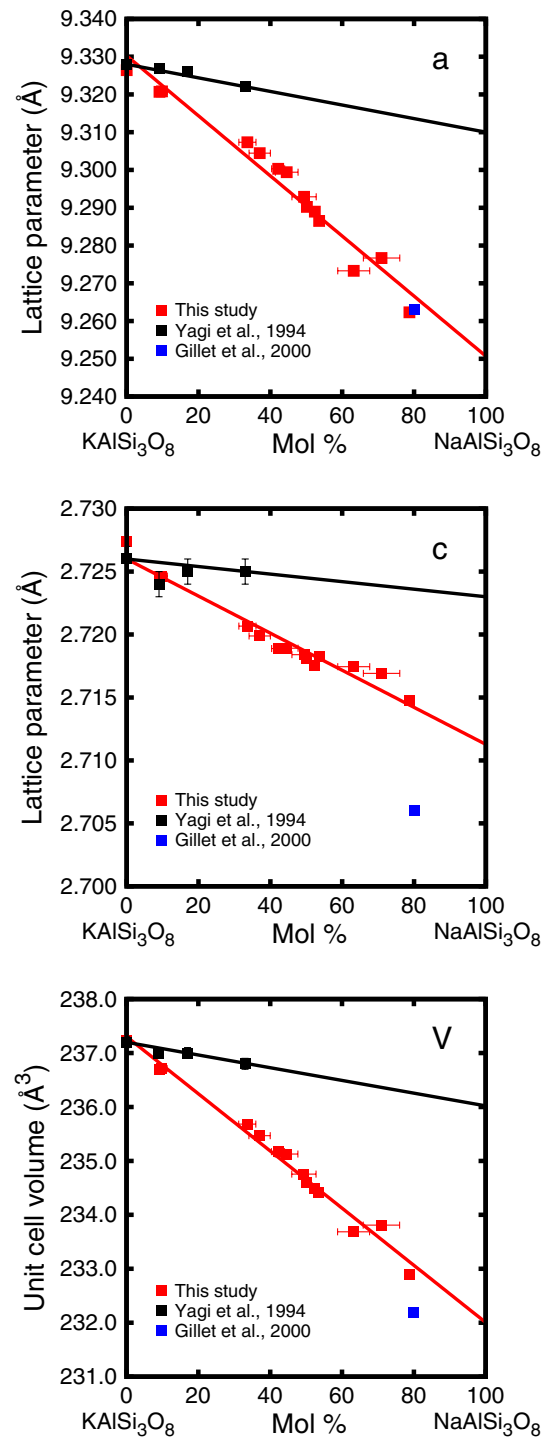


Fig. 4 Lattice parameters and unit cell volumes of hollandite. Vertical error bars of our data points are shorter than the vertical size of the square symbols

The length of its a axis matches our results, while that of its c axis is obviously smaller, which is likely attributed to the additional substitution of Si by Al for the incorporation of Ca in the hollandite structure.

Phase relations determined via static high-pressure experiments can be used to constrain the shock P–T conditions of meteorites. Typically, the phase assemblage of aluminous garnet plus magnesiowüstite as the matrix of shock veins constrains P–T conditions at 20–25 GPa and 2273–2500 K (Chen et al. 1996; Ohtani et al. 2004; Xie et al. 2006; Ozawa et al. 2009), according to the melting phase relations of the KLB-1 peridotite (Zhang and Herzberg 1994) and the Allende meteorite (Agee et al. 1995). Lingunite likely occurred at P–T conditions similar to those of the shock veins (20–25 GPa and 2273–2500 K), as suggested by the stability region of $K_{0.2}Na_{0.8}AlSi_3O_8$ hollandite at 22 GPa and 2273 K. However, compared with the composition of $K_{0.2}Na_{0.8}AlSi_3O_8$, the typical composition of lingunite, $Ab_{85}An_{10}Or_5$ (Ab, albite; An, anorthite; Or, orthoclase) (e.g., Gillet et al. 2000; Tomioka et al. 2000), contains less K, which leads to a higher Na/(K + Na) ratio (about 0.94). As indicated in Fig. 3c, hollandite with Na/(K + Na) ratios higher than 0.8 (Na contents higher than 80 mol%) is likely stable around 22 GPa only above 2273 K. This suggests that the formation of lingunite needs temperatures higher than 2273 K. On the other hand, it is shown in Fig. 3b that the stability region of $K_{0.2}Na_{0.8}AlSi_3O_8$ hollandite is quite narrow at 2273 K, about 0.5 GPa around 22 GPa. Even the phase boundaries representing the solubility of Na in hollandite likely shift toward a Na-rich direction with further increasing temperature above 2273 K, as indicated in Fig. 3c, the stability region of hollandite with Na contents higher than 80 mol% unlikely spans a wide range of pressure. Thus, the occurrence of lingunite in the shock veins of strongly shocked meteorites constrains the shock P–T conditions to pressures around 22 GPa and temperatures above 2273 K, which should be further explored with considering the effect of Ca on the stability of lingunite.

Acknowledgments The authors are grateful to Dr. Kiyoshi Fujino, Dr. Toru Inoue, Dr. Yu Nishihara, Dr. Takeshi Sakai and Dr. Vincenzo Stagno for their discussion and comments. The authors are also grateful to the anonymous reviewers for their comments and advices.

References

- Agee CB, Li J, Shannon MC, Circone S (1995) Pressure-temperature phase diagram for the Allende meteorite. *J Geophys Res* 100:17725–17740. doi:10.1029/95JB00049
- Akaogi M, Ajiro H, Kojitani H (2005) High-pressure phase relations of hollandite in the system $KAlSi_3O_8$ – $NaAlSi_3O_8$. In: 2005 Annual meeting of the mineralogical society of Japan, Session ID K1-03. doi:10.14824/kobutsu.2005.0.3.0
- Akaogi M, Haraguchi M, Nakanishi K, Ajiro H, Kojitani H (2010) High-pressure phase relations in the system $CaAl_4Si_2O_{11}$ – $NaAl_3Si_3O_{11}$ with implication for Na-rich CAS phase in shocked Martian meteorites. *Earth Planet Sci Lett* 289:503–508. doi:10.1016/j.epsl.2009.11.043
- Boffa Ballaran T, Liu J, Dubrovinsky LS, Caracas R, Crichton W (2009) High-pressure ferroelastic phase transition in aluminosilicate hollandite. *Phys Rev B* 80:214104. doi:10.1103/PhysRevB.80.214104
- Caracas R, Boffa Ballaran T (2010) Elasticity of (K, Na) $AlSi_3O_8$ hollandite from lattice dynamics calculations. *Phys Earth Planet Inter* 181:21–26. doi:10.1016/j.pepi.2010.04.004
- Chen M, Sharp TG, El Goresy A, Wopenka B, Xie X (1996) The majorite-pyrope + magnesiowüstite assemblage: constraints on the history of shock veins in chondrites. *Science* 271:1570–1573. doi:10.1126/science.271.5255.1570
- Fei Y, Orman JV, Li J (2004) Experimentally determined postspinel transformation boundary in Mg_2SiO_4 using MgO as an internal pressure standard and its geophysical implications. *J Geophys Res* 109:B02305. doi:10.1029/2003JB002562
- Ferroir T, Onozawa T, Yagi T et al (2006) Equation of state and phase transition in $KAlSi_3O_8$ hollandite at high pressure. *Am Mineral* 91:327–332. doi:10.2138/am.2006.1879
- Gillet P, Chen M, Dubrovinsky L, El Goresy A (2000) Natural $NaAlSi_3O_8$ -hollandite in the shocked Sixiangkou meteorite. *Science* 287:1633–1636. doi:10.1126/science.287.5458.1633
- Ishii T, Kojitani H, Akaogi M (2012) High-pressure phase transitions and subduction behavior of continental crust at pressure-temperature conditions up to the upper part of the lower mantle. *Earth Planet Sci Lett* 357–358:34–41. doi:10.1016/j.epsl.2012.09.019
- Kawai K, Tsuchiya T (2013) First-principles study on the high-pressure phase transition and elasticity of $KAlSi_3O_8$ hollandite. *Am Mineral* 98:207–218. doi:10.2138/am.2013.4077
- Liu L (1978) High-pressure phase transformations of albite, jadeite and nepheline. *Earth Planet Sci Lett* 37:438–444. doi:10.1016/0012-821X(78)90059-6
- Liu X (2006) Phase relations in the system $KAlSi_3O_8$ – $NaAlSi_3O_8$ at high pressure–high temperature conditions and their implication for the petrogenesis of lingunite. *Earth Planet Sci Lett* 246:317–325. doi:10.1016/j.epsl.2006.04.016
- Liu L, El Goresy A (2007) High-pressure phase transitions of the feldspars, and further characterization of lingunite. *Int Geol Rev* 49:854–860. doi:10.2747/0020-6814.49.9.854
- Liu J, Boffa-Ballaran T, Dubrovinsky L, Frost D (2005) High pressure study of K–Na hollandite solid solution. In: American Geophysical Union, Fall Meeting 2005, Abstract No. MR31A-0125
- Ma C, Tschauer O, Beckett JR, Rossman GR (2015) Liebermannite: a new potassic hollandite ($KAlSi_3O_8$) from the Zagami basaltic shergottite. In: 46th Lunar and Planetary Science Conference, LPI Contribution No. 1832. p 1401
- Morishima H, Kato T, Suto M et al (1994) The phase boundary between α - and β - Mg_2SiO_4 determined by in situ X-ray observation. *Science* 26:1202–1203. doi:10.1126/science.265.5176.1202
- Nishiyama N, Rapp RP, Irifune T, Sanehira T, Yamazaki D, Funakoshi K (2005) Stability and P–V–T equation of state of $KAlSi_3O_8$ -hollandite determined by in situ X-ray observations and implications for dynamics of subducted continental crust material. *Phys Chem Miner* 32:627–637. doi:10.1007/s00269-005-0037-y
- Ohfuji H, Yamamoto M (2015) EDS quantification of light elements using osmium surface coating. *J Mineral Petrol Sci* 110:189–195. doi:10.2465/jmps.141126
- Ohtani E, Kimura Y, Kimura M, Takata T, Kondo T, Kubo T (2004) Formation of high-pressure minerals in shocked L6 chondrite Yamato 791384: constraints on shock conditions and parent body size. *Earth Planet Sci Lett* 227:505–515. doi:10.1016/j.epsl.2004.08.018
- Ozawa S, Ohtani E, Miyahara M, Suzuki A, Kimura M, Ito Y (2009) Transformation textures, mechanisms of formation of high-pressure minerals in shock melt veins of L6 chondrites, and pressure-temperature conditions of the shock events. *Meteorit Planet Sci* 44:1771–1786. doi:10.1111/j.1945-5100.2009.tb01206.x

- Ringwood AE, Reid AF, Wadsley AD (1967) High-pressure KAlSi_3O_8 , an aluminosilicate with sixfold coordination. *Acta Crystallogr* 23:1903–1905. doi:[10.1107/S0365110X6700430X](https://doi.org/10.1107/S0365110X6700430X)
- Stöffler D, Keil K, Edward S (1991) Shock metamorphism of ordinary chondrites. *Geochim Cosmochim Acta* 55:3845–3867. doi:[10.1016/0016-7037\(91\)90078-J](https://doi.org/10.1016/0016-7037(91)90078-J)
- Sueda Y, Irifune T, Nishiyama N et al (2004) A new high-pressure form of KAlSi_3O_8 under lower mantle conditions. *Geophys Res Lett* 31:L23612. doi:[10.1029/2004GL021156](https://doi.org/10.1029/2004GL021156)
- Suzuki A, Ohtani E, Morishima H et al (2000) In situ determination of the phase boundary between wadsleyite and ringwoodite in Mg_2SiO_4 . *Geophys Res Lett* 27:803–806. doi:[10.1029/1999GL008425](https://doi.org/10.1029/1999GL008425)
- Tomioka N, Mori H, Fujino K (2000) Shock-induced transition of $\text{NaAlSi}_3\text{O}_8$ feldspar into a hollandite structure in a L6 chondrite. *Geophys Res Lett* 27:3997–4000. doi:[10.1029/2000GL008513](https://doi.org/10.1029/2000GL008513)
- Tutti F (2007) Formation of end-member $\text{NaAlSi}_3\text{O}_8$ hollandite-type structure (lingunite) in diamond anvil cell. *Phys Earth Planet Inter* 161:143–149. doi:[10.1016/j.pepi.2007.02.004](https://doi.org/10.1016/j.pepi.2007.02.004)
- Urakawa S, Kondo T, Igawa N, Shimomura O, Ohno H (1994) Synchrotron radiation study on the high-pressure and high-temperature phase relations of KAlSi_3O_8 . *Phys Chem Miner* 21:387–391. doi:[10.1007/BF00203296](https://doi.org/10.1007/BF00203296)
- Xie Z, Sharp TG, DeCarli PS (2006) High-pressure phases in a shock-induced melt vein of the Tenham L6 chondrite: constraints on shock pressure and duration. *Geochim Cosmochim Acta* 70:504–515. doi:[10.1016/j.gca.2005.09.003](https://doi.org/10.1016/j.gca.2005.09.003)
- Yagi A, Suzuki T, Akaogi M (1994) High pressure transitions in the system KAlSi_3O_8 – $\text{NaAlSi}_3\text{O}_8$. *Phys Chem Miner* 21:12–17. doi:[10.1007/BF00205210](https://doi.org/10.1007/BF00205210)
- Yamada H, Matsui Y, Ito E (1984) Crystal-chemical characterization of KAlSi_3O_8 with the hollandite structure. *Mineral J* 12:29–34. doi:[10.2465/minerj.12.29](https://doi.org/10.2465/minerj.12.29)
- Zhang J, Herzberg C (1994) Melting experiments on anhydrous peridotite KLB-1 from 5.0 to 22.5 GPa. *J Geophys Res* 99:17729–17742. doi:[10.1029/94JB01406](https://doi.org/10.1029/94JB01406)